

Short Communication

Effect of Zeta Potential and Particle Size on the Stability of SiO₂ Nanospheres as Carrier for Ultrasound Imaging Contrast Agents

Di Sun¹, Shifei Kang², Chenglu Liu², Qijie Lu¹, Lifeng Cui^{2,*}, Bing Hu^{1,*}

¹ Department of Ultrasound in Medicine, Shanghai Jiao tong University Affiliated sixth People's Hospital, Shanghai Institute of Ultrasound in Medicine, Shanghai 200233, China

² Department of Environmental Science and Engineering, University of Shanghai for Science and Technology, Shanghai 200093, China

*E-mail: binghu_zz@163.com, lifeng.cui@gmail.com

Received: 7 July 2016 / Accepted: 9 August 2016 / Published: 6 September 2016

A series of SiO₂ nanospheres (NPs) and amino-functionalized SiO₂ NPs were synthesized through a modified Stöber method and eventually used as the model of SiO₂ carrier for ultrasound imaging contrast agents loading. The physicochemical properties of these materials were characterized by X-ray diffractometry (XRD), transmission electron microscopy (TEM) and Fourier transform infrared detector (FT-IR). Also, the zeta potential and diameter of the as-prepared SiO₂ NPs was measured and compared. It can be observed that the particle size of obtained SiO₂ spheres are controllable from 100 nm to 800 nm by adjusting the synthetic condition. SiO₂ NPs size 200 nm and 400 nm exhibit remarkable uniformity, while the morphology of ~800 SiO₂ spheres turns to irregular. The zeta potential of the unmodified SiO₂ NPs was much higher than conventional carriers of ultrasound imaging contrast agents, indicating that the monodisperse stability of small SiO₂ NPs was superior. After amino-function, SiO₂ NPs size ~400 nm show the highest zeta potential of -45.5 mV, which will benefit the carrier transportation when it pass though the endothelial barriers of tumour tissue. The excellent stability and unique surface groups of amino-modified SiO₂ NPs will significantly benefit the loading of drugs and biological ligands, thus show insight for its future applications of nanomedicine and clinical ultrasound imaging beyond blood vessel.

Keywords: Ultrasound imaging contrast agents, SiO₂, Zeta potential, Size control

1. INTRODUCTION

Currently, the early specific imaging diagnosis of tumours is one of the most important goals of modern nanomedicine, which permit the subsequent comprehensive diagnosis and appropriate

treatment of the diseases. Imaging contrast agents with targeted function, which must be constructed by combined functional imaging contrast agents and their carrier, can meet the requirements of modern molecular imaging, thus plays a crucial role in the hot spot of tumours imaging[1]. Among all the early imaging diagnosis method for diseases, due to its unique advantages such as safe, fast, cheap and non-invasive, ultrasound imaging (US) has been widely used as a promising clinical imaging modality[2]. In vivo, solid media and gas cavity appears with different gray level by ultrasound refraction, thus high-resolution ultrasound photos can be obtained. As the same as other medicine imaging techniques, ultrasound imaging contrast agents (usually gas microbubbles) was also crucial in clinical diagnosis. In fact, contrast-enhanced ultrasound imaging (CEUS) technique, which using fluorocarbon microbubbles as the main contrast agents, have been developed to be one of the most popular and effective imaging diagnosis methods of tumours[3]. Unfortunately, the stability of these fluorocarbon gas microbubbles were quite limited (usually collapse within seconds after injection into the bloodstream) because of Laplace pressure and ultrasound explosion[4]. Therefore, the nanosized encapsulated liquid fluorocarbon ultrasound imaging contrast agents is attractive, which can generate gas microbubbles under trigger energy after be transformed into tumour sites. Only under the protection of an appropriate carrier can liquid fluorocarbon keep stable under blood pressure and oxygen metabolism impression during transport process, then serve as acoustic-sensitive contrast agents. Furthermore, contrast agents carriers can be linked with various of functional groups (such as $-NH_2$ or $-OH$), fluorescent molecules and biological ligands, which is essential for target imaging diagnosis of tumours.

For decades, many carrier materials have been investigated for targeted ultrasound imaging. Traditionally, gas-filled microbubbles encapsulated by soft-shell carriers made of polymers[5] and lipids[6], have been developed and used clinically. Though microbubbles contrast agents carried by organic soft-shell carriers can enhance the ultrasound signal, due to their large particles sizes ($\sim 5\mu m$) and broad size distribution, they can persist for only 15 min in blood, not to mention the potential to pass through endothelial barriers[7]. Moreover, all currently used soft-shell encapsulated microbubbles can hardly be functionalized with targeting ligands, thus the accumulate at tumour sites was not easy. Because the above limitations, it is of great significance to develop new kinds of carriers for precise target tumour imaging and therapy. In this regard, inorganic nanoparticles carriers, especially silica NPs carriers, are receiving increasing attention due to their corrosion resistance features and high chemical stability in vivo[8,9]. For years, silica nanoparticles drug carriers are believed to be "generally recognized as safe" by the Food and Drug Administration of the USA[10]. Moreover, silica nanoparticles have been considered as one of the most biocompatible carrier for contrast enhancing agents of US imaging and have been successfully exploited in clinical US imaging diagnosis[11].

However, despite the examples described above, the uses of silica-based nanoparticles as carrier of contrast enhancing agents are only in a preclinical development stage. Up to now, there are few reports focus on the relationship of surface zeta potential with the particle size of SiO_2 NPs for ultrasound imaging contrast agents, which is decisive on the stability and functional potential of target transportation and drug loading for clinical imaging. More importantly, the particles size of most of the reported silica nanoparticles are too large to go through the gap of capillary vessel, which means they can only serve as in vessel but not in tumour. Therefore, it is important to synthesize SiO_2 NPs with

appropriate size and controllable surface zeta potential as imaging contrast agents to achieve high-resolution ultrasound imaging beyond blood vessel.

In this work, a simple self-seeding approach to prepare the spherical SiO₂ was reported. The traditional Stöber method for synthesis of SiO₂ NPs was improved to reliably control the particles size and uniformity of SiO₂ NPs. Amino-group was also introduced to functionalized SiO₂ NPs thus increase the charge on the surface. The particles size distribution from TEM and Laser Zeta meter tests, as well as monodisperse stability reflected by zeta potential was calculated and compared. Additionally, the potential of SiO₂ NPs carrier in future applications of nanomedicine and clinical ultrasound imaging was discussed.

2. EXPERIMENTAL

Chlorotrimethylsilane and tetraethyl orthosilicate (TEOS) were purchased from Sigma-Aldrich Co., Ltd. All other reagents were purchased from Shanghai Chemical Co., Ltd. All chemicals involved were analytical reagent (AR) grade and used as received without further purification.

Monodisperse SiO₂ nanospheres were prepared by a simple self-seeding approach based on traditional Stöber method[12]. In a typical procedure, SiO₂ spheres with an average diameter of ~200 nm were prepared by mixing a premixed solution consisted of ethanol (50 mL), ammonia (10 mL) and deionized water (30 mL) with a TEOS solution (TEOS 10 mL, ethanol 50 mL) under stirring at 25 °C for 2 h. The obtained silica nanospheres were washed with water three times and dried at 60 °C for 3 h. SiO₂ spheres with an average diameter of ~400 nm were prepared though the same way except for using the same amount of the ~200 nm SiO₂ spheres mixture instead of TEOS. In turn, the ~400 nm SiO₂ sphere sample was used as seeds for the growth of ~800 nm SiO₂ spheres in the same liquid environment. The obtained nonporous silica spheres was designated as SNP-200, SNP-400 and SNP-800, respectively. The amino-functionalized SiO₂ NPs were prepared according to the procedure reported previously[13]. Typically, 1.0 g of SiO₂ NPs was soaked in a 10 g methanol solution containing 0.67 g TEPA at room temperature for 3 h, then dried at 45 °C under reduced pressure overnight to evaporate methanol and avoid amino group degradation. The resulting hybrid materials were designated as ASNP-200, ASNP-400 and ASNP-800, respectively, and the TEPA weight percentage in the hybrid materials was about 5 %.

The morphology of the samples was examined by a transmission electron microscope (TEM, JEOL JEM-2010) at an acceleration voltage of 200 kV. The value of the zeta potential and diameter distribution of the samples was determined using Laser Zeta meter (Malvern Instruments, Zetasizer Nano ZS 90) in water solution (PH=7.4). The crystal structural of the unmodified SiO₂ NPs were investigated on a Bruker D8 Advance X-ray diffractometer (XRD) with Cu-K α radiation, operated at 40 kV and 40 mA (scanning step: 0.02°/s) in the 2 θ range of 10-80°. The amino-function effect of the amino-modified SiO₂ NPs was determined by a Fourier transform infrared (FTIR) spectra (Nicolet Nexus 470).

3. RESULTS AND DISCUSSION

Figure 1 showed the TEM images of the obtained SiO₂ spheres with different particle size. Figure 1a-b indicated that the ~200 nm SiO₂ nanospheres were spherical and highly monodispersed, the diameter of SNP-200 nanospheres was about 221 nm and the relative deviation was about 8.6%. Figure 1c-d indicated that the ~400 nm SiO₂ NPs were also spherical and highly monodispersed, the diameter of SNP-400 NPs was about 432 nm and the relative deviation was about 9.6%. The surface of SNP-200 and SNP-400 spheres was clean, and no visible pores can be observed. However, as shown in Figure 1e-f, the ~800 nm SiO₂ spheres turn irregular and a lot of small particles appear. The diameter of SNP-800 spheres was about 788 nm and the relative deviation increased to 32.6%.

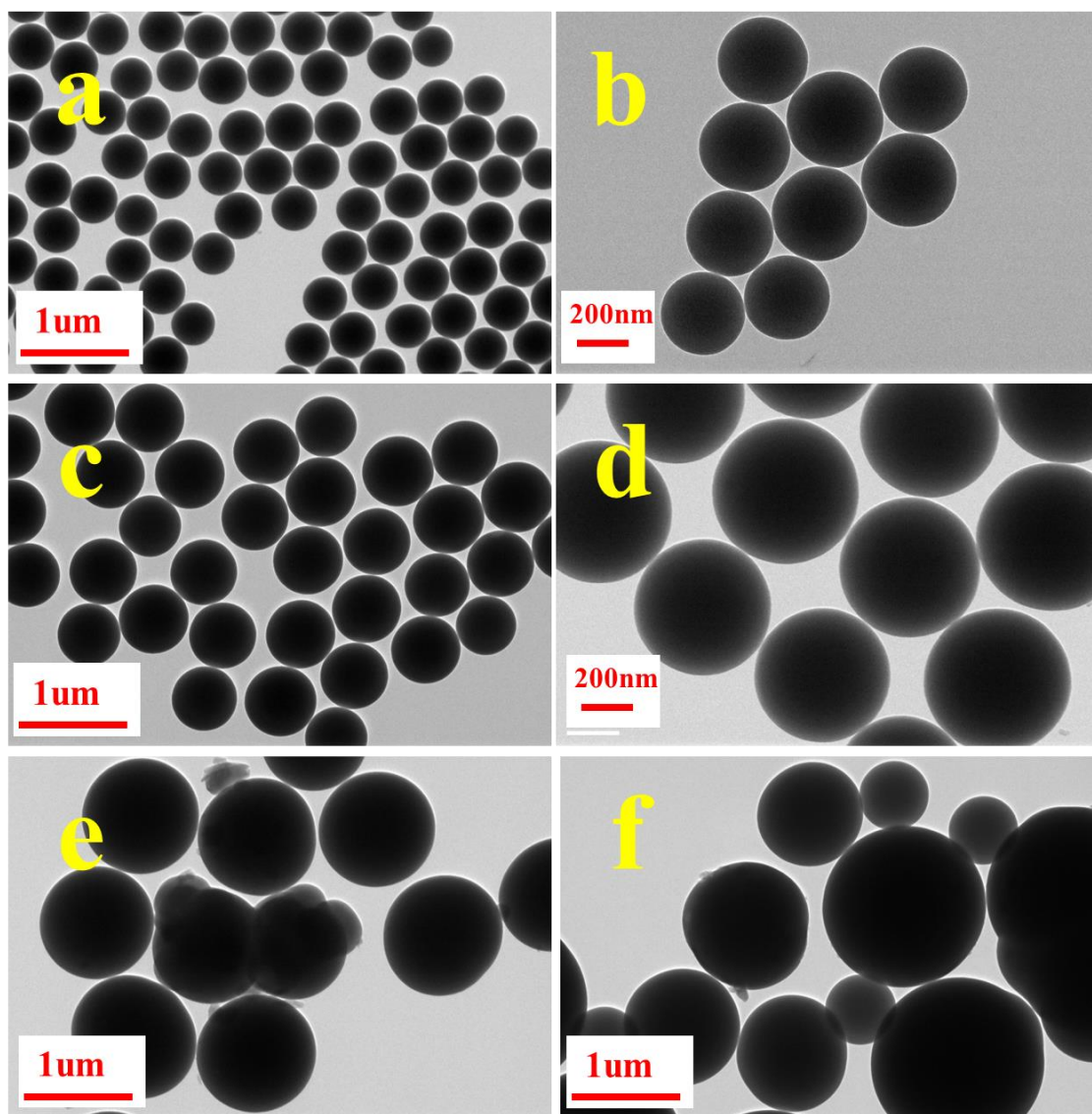


Figure 1. TEM images of SiO₂ NPs with different particle size, (a-b) ~200 nm, (c-d) ~ 400 nm, (e-f) ~800nm.

In comparison with the unmodified SiO₂ NPs, as shown in Figure 2a and Figure 2b, the ~400

nm SiO₂ particles modified by amino-functionalized were also spherical, and the diameter keeps almost the same with that of the unmodified ones. It can be observed from Figure 2b that the surface turns rough after amino-modification, this can be ascribed to the loading of TEPA related amino-groups. No obvious conglutination or agglomeration can be observed, indicating the amino-functionalized do not damage to the highly uniform morphology of SiO₂ spheres substrate.

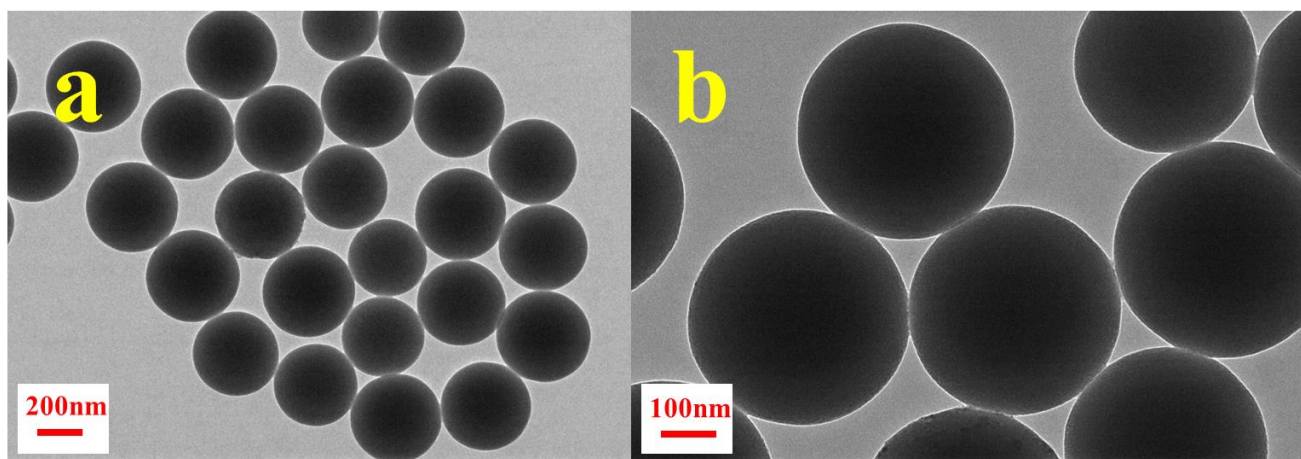


Figure 2. TEM images of amino functionalized ~400 nm SiO₂ NPs.

The average diameter of the obtained SiO₂ spheres from TEM and laser particle size measurement were calculated and compared, all the data was list in Table 1. Because of the laser scattering during laser measuring process, the average diameter of the obtained SiO₂ spheres calculated by laser particle size measurement was larger than that calculated from TEM. The average diameter of the SiO₂ NPs increased slightly after amino-modification by laser particle size measurement, while keeping almost the same with that of the unmodified samples. This enlarged particle size can be ascribed to the TEPA related amino groups, which did not enlarge the solid size of amino-modified SiO₂ NPs, but can serve to widen the electric double layer surrounding SiO₂ NPs and enhance the laser scattering, thus caused to a larger calculated average diameter by laser zeta meter instrument.

The particle size distribution and relative deviation of the obtained SiO₂ spheres in this work was in accordance with former reported SiO₂ NPs based on Stöber method. It is well know that SiO₂ spheres in a wide sub-micrometer diameter range can be synthesized by the Stöber method. The particles size change of SNP in Stöber system is reliable and has been discussed intensively by many papers[14]. Besides, the size of the SiO₂ NPs is controlled by the parameters influencing the colloidal stability, i.e., ionic strength, pH, charge on the particles, temperature, solvent viscosity, and dielectric constant of the solvent[15-18]. The proposed formation mechanism leads to improved control of the particle characteristics relevant to this work. In a typical process, spherical SiO₂ particles are prepared by the hydrolysis and condensation of TEOS in a mixture of ethanol, water, and ammonia. Subsequently, this intermediate reaction product condenses eventually to form spherical SiO₂ particles. The electric double layer was formed surrounding every single SiO₂ spheres because of the ionization of -OH on the surface of silica in the ethanol solution. The width of the electric double layer, which can be reflects by zeta potential measurement, have determinative effects on the relative diameter deviation of SiO₂ particles. In this regard, the zeta potential which can describe the nanomaterials

distribution stability state is a useful parameter to evaluate the adsorption potential of drugs on the nanomaterials surfaces, since it reflects the electrostatic interactions of drugs on the nanomaterials surfaces.

The zeta potential of the obtained SiO₂ spheres in water (PH=7.4) was also listed in Table 1. Because can be used to evaluate the stability of colloidal systems, zeta potential is very important parameters which reflect their potential as carrier of ultrasound imaging contrast agents, which needs to be inert thus easy to trace and remove during in-vivo using process. It is well known that higher absolute value of zeta potential means higher stable state of colloidal systems, and potential values higher than +30 mV or lower than -30 mV permits a basically stable suspension[19,20]. Furthermore, zeta potential data not only reflect the stability of colloidal systems of the SNP dispersion in water, but also have been used to explain the adsorption mechanisms of drugs and biological ligands on the surface of SNP[21-23]. According to the zeta potential values of the SiO₂ spheres listed in Table 1, all the SiO₂ spheres obtained show a favorable negative zeta potential value. Before modification, the zeta potential values of the SiO₂ spheres decreased when particle size increased, especially for the ~800 nm SiO₂ spheres. The reason can be ascribed to the disordered self-seeding growth caused morphology changes of SiO₂ spheres, which can be observed in TEM results. After modification, due to the amino group related boarded electric double layer surrounding SiO₂ NPs, the zeta potential values of the SiO₂ NPs with different particle size all increased. The SNP-400 sample reveals the most prominent increase in zeta potential value (-37.7 mV to -45.5 mV) as represented in Fig.5, mainly because of the proper particle numbers, which can avoid too much electric double layer interaction when particle numbers were high. The higher zeta potential value of ASNP-400 indicated the excellent stability of SiO₂ NPs under amino-modification treatment. Moreover, the negative charges on the surface of SiO₂ NPs are important for static interaction with biological ligands and ultrasound imaging contrast agents, most of which were cationic. Thus the loading efficiencies and stability of drugs using as-prepared SiO₂ NPs was promising. The amide groups act as neutral functional groups to maintain and strengthen the negative charges on the surface of SiO₂ NPs, which was the key factor for dispersibility of SiO₂ NPs in water. The effect of pH on the zeta potential is not investigated here because the actual using environment of SNP is in-vivo, thus the investment at PH 7.4 is enough, which is close to the PH of blood and most tissues.

Table 1. The zeta potential and calculated average diameter of the obtained SiO₂ spheres.

Sample	Zeta potential (mV)	average diameter calculated by laser particle size measurement (nm)	Average Diameter calculated from TEM (nm)
SNP-200	-39.1	243	221
SNP-400	-37.7	465	432
SNP-800	-31.0	823	788
ASNP-200	-41.5	254	222
ASNP-400	-45.5	488	432
ASNP-800	-32.9	845	787

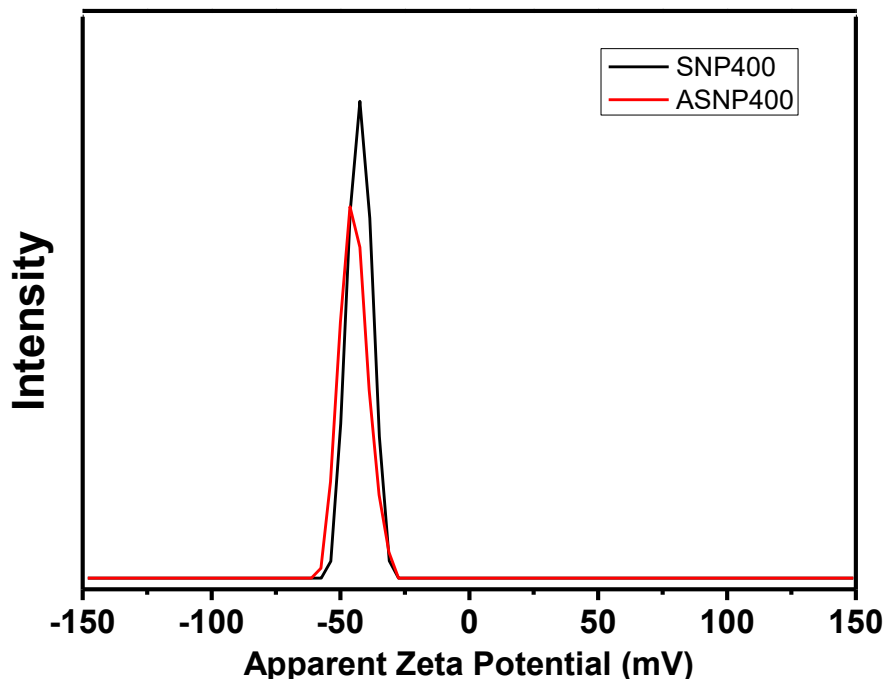


Figure 3. Zeta potential of the obtained SNP-400 and ASNP-400 samples.

X-ray diffractometry was used to determine the crystal structure of SiO₂ NPs. Figure 4 shows the X-ray diffraction pattern of unmodified SiO₂ NPs, respectively. XRD patterns of all the SNP samples have a wide hump in the range of 2θ from 16° to 30°, typical for amorphous silica[24]. No peak assigned to silica crystal appeared, suggesting that the all the silica samples obtained were amorphous[25].

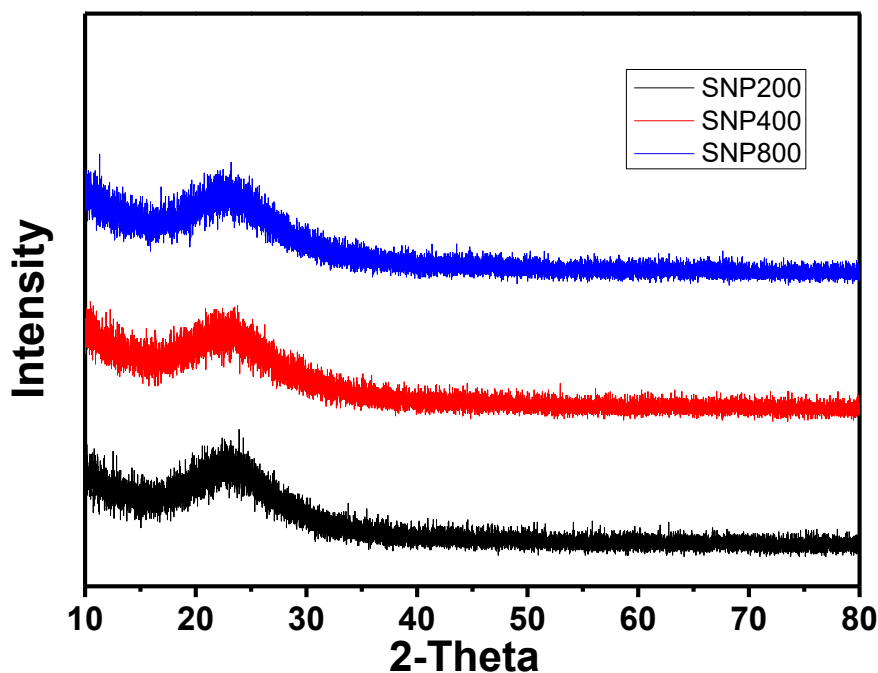


Figure 4. XRD pattern of unmodified SiO₂ NPs.

The FT-IR spectra of SNP-400 and ASNP-400 are shown in Fig. 5 to investigate the amino-function effect. Spectra of both samples appeared a broad and strong band at around 472 cm^{-1} , 799 cm^{-1} , and 1091 cm^{-1} , which were characteristic bands of the Si-O-Si symmetric stretching vibration and asymmetric stretching vibration[27]. The Si-O-Si vibrations indicated a typical silica surface of obtained samples before and after modification. The bands at 1237 cm^{-1} , 1579 cm^{-1} and 1671 cm^{-1} are associated with the stretching vibration of C-N and the bending vibration of N-H from TEPA[27], respectively, which demonstrates that TEPA was successfully impregnated into the support. Successful amino-functionalization of the silica surface on SNP-400 was also evidenced by the absorption at 3390 cm^{-1} , which can be assigned to the stretching and bending vibrations of uncondensed terminal amino groups as well[28]. The absorption peaks at about 1237 cm^{-1} , 1671 cm^{-1} and 3390 cm^{-1} of SNP-400 sample can be ascribed to the ammonia remains during preparation process. These FT-IR results above verified the successful preparation of designed amino-functionalized SiO_2 NPs.

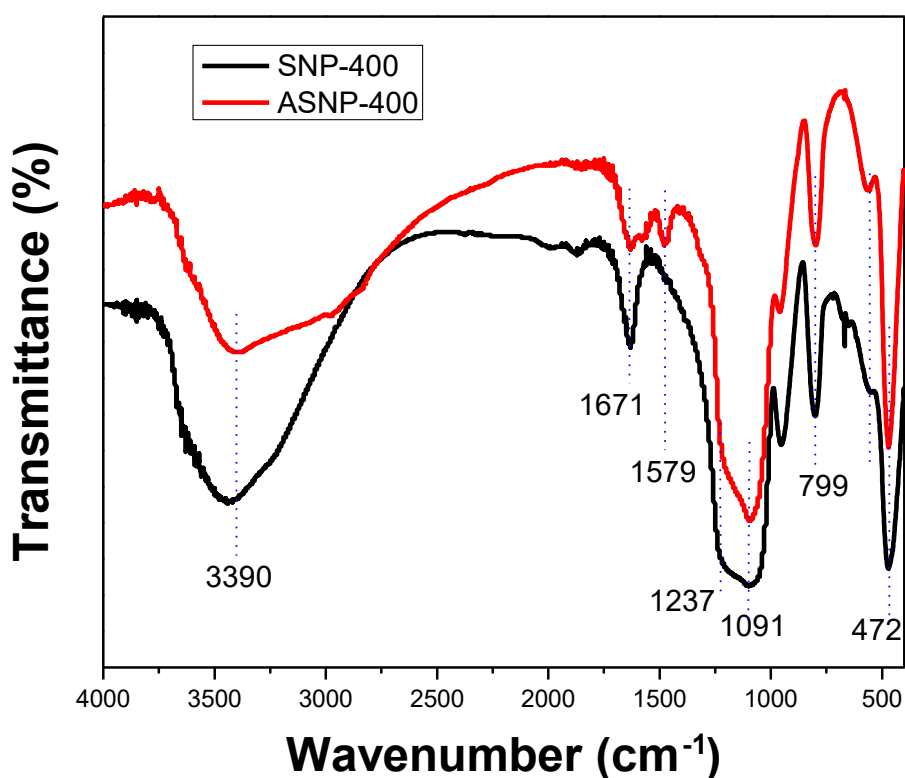


Figure 5. FT-IR spectra of SNP-400 and ASNP-400 samples.

In summary, a series of silica nanospheres with different particle size and surface property was characterized toward the design of multifunctional carrier of ultrasound imaging contrast agents. The self-seeding approach to prepare size-controllable spherical was proved to be practical. The FT-IR spectra indicated the successful. Among all of the obtained samples, ASNP-400 with a $\sim 400\text{ nm}$ diameter shows the superior zeta potential value, the particle size match the size requirement perfectly for SNP to pass through the endothelial barriers of tumour tissue while cannot pass through the endothelial barriers of normal tissue, thus can be used in ultrasound imaging applications beyond blood

vessel. Moreover, the decent zeta potential value will benefit the loading of drugs and biological ligands in SiO₂ carriers significantly thus brings insight for its future applications of nanomedicine and clinical ultrasound imaging.

4. CONCLUSION

In conclusion, controllable synthesis of SiO₂ nanospheres with the diameter range 200-800nm was realized by a simple self-seeding approach based on classic Stöber method. The as-prepared amorphous silica NPs show highly uniform spherical morphology before and after amino-modification. FT-IR spectra demonstrated the successful grafting of amino-group to SiO₂ spheres, which is favorable for subsequently drugs loading. The negative surface zeta potential of all silica NPs was recorded, the amino-functionalized SNP-400 spheres show the highest absolute zeta potential value of 45.5 mV, indicating the excellent stability of SiO₂ NPs after amino-modification. The ~400 nm diameter of ASNP-400 spheres meet the ideal carrier particle size requirements in ultrasound imaging applications, which can exactly pass through the endothelial barriers of tumour tissue while cannot pass through normal tissue, thus can be used in beyond blood vessel. The decent zeta potential value and appropriate particle size make the chosen sample promising in future applications as multifunctional nanoplatform for both ultrasound imaging diagnostic and therapeutic purposes.

ACKNOWLEDGEMENTS

This work was supported by National Natural Science Foundation of China (Grant No. 81271597 and 51502172).

References

1. K. Riehemann, S. W. Schneider, T. A. Luger, B. Godin, M. Ferrari, H. Fuchs, *Angew Chem Int Edit* 48 (2009) 872-897.
2. H. D. Liang, M. J. K. Blomley, *Brit J Radiol* 76(2003) S140-S150.
3. D. Sun, C. Wei, E. Shen, T. Ying, B. Hu, *Sci. Rep.* 6 (2016), 29303.
4. E. G. Schutt, D. H. Klein; R. M. Mattrey; J. G. Riess, *Angew Chem Int Edit* 42 (2003) 3218-3235.
5. R. Diaz-Lopez, N. Tsapis, M. Santin, S. L. Bridal, V. Nicolas, D. Jaillard, D. Libong, P. Chaminade, V. Marsaud, C. Vauthier, E. Fattal, *Biomaterials* 31 (2010) 1723-1731.
6. S. Hernot, A. L. Klibanov, *Adv Drug Deliver Rev* 60 (2008) 1153-1166.
7. J. M. Hyvelin, I. Tardy, T. Bettinger, M. V. Wronski, M. Costa, P. Emmel, D. Colevret, P. Bussat, A. Lassus, C. Botteron, A. Nunn, P. Frinking, F. Tranquart, *Invest Radiol* 49(2014) 224-235.
8. P. Yang, F. Wang, X. F. Luo, Y. T. Zhang, J. Guo, W. B. Sho, C. C. Wang, *Acs Appl Mater Inter* 6 (2014) 12581-12587.
9. A. Liberman, Z. Wu, C. V. Barback, R. Viveros, S. L. Blair, L. G. Ellies, D. R. Vera, R. F. Mattrey, A. C. Kummel, W. C. Trogler, *Acs Nano* 7 (2013) 6367-6377.
10. C. Caltagirone, A. Bettoschi, A. Garau, R. Montis, *Chem Soc Rev* 44 (2015) 4645-4671.
11. J. Liu, A. L. Levine, J. S. Mattoon, M. Yamaguchi, R. J. Lee, X. L. Pan, T. J. Rosol, *Phys Med Biol* 51 (2006) 2179-2189.
12. Q. S. Qu, Y. Min, L. H. Zhang, Q. Xu, Y. D. Yin, *Anal Chem* 87 (2015) 9631-9638.
13. X. Wang, L. L. Chen, Q. J. Guo, *Chem Eng J* 260 (2015) 573-581.
14. L. Y. Liu, X. F. Wang, B. Cheng, C. X. Zhang, *J Brazil Chem Soc* 20 (2009) 46-50.

15. W. Stöber, A. Fink, E. Bohn, *J Colloid Interface Sci* 26 (1968) 62–69
16. N. Plumere, A. Ruff, B. Speiser, V. Feldmann, H.A. Mayer, *J Colloid Interf Sci* 368 (2012) 208-219.
17. H.X. Gong, N. Li, Y.T. Qian, *Int J Electrochem Sc* 8 (2013) 9811-9817.
18. X.Y. Guo, F.F. Mao, W.J. Wang, Y. Yang, Z.M. Bai, *Acs Appl Mater Inter* 7 (2015) 14983-14991.
19. P. Wang, A. A. Keller, *Langmuir* 25 (2009) 6856-6862.
20. E.F. de la Cruz, Y.D. Zheng, E. Torres, W. Li, W.H. Song, K. Burugapalli, *Int J Electrochem Sc* 7 (2012) 3577-3590.
21. A. E. Wiacek, *Powder Technol* 213 (2011) 141-147.
22. A.M. Atta, H.A. Al-Lohedan, Z.A. ALOThman, A.M. Tawfeek, A. AbdelGhafar, N.A. Hamad, *Int J Electrochem Sci.*, 11 (2016) 3786-3802.
23. S. Salgin, U. Salgin, S. Bahadir, *Int J Electrochem Sc* 7 (2012) 12404-12414.
24. Z. M. Sun, C. H. Bai, S. L. Zheng, X. P. Yang, R. L. Frost, *Appl Catal a-Gen* 458 (2013) 103-110.
25. S. E. Fritz, S. M. Martin, C. D. Frisbie, M. D. Ward, M. F. Toney, *J Am Chem Soc* 126 (2004), 4084-4085.
26. S. Y. Bao, L. H. Tang, K. Li, P. Ning, J. H. Peng, H. B. Guo, T. T. Zhu, Y. Liu, *J Colloid Interf Sci* 462 (2016) 235-242.
27. A. Nikolic, B. Jovic, V. Krstic, J. Trickovic, *J Mol Struct* 889 (2008) 328-331.
28. S. Kang, Y. Fang, Y. Huang, L. F. Cui, Y. Wang, H. Qin, Y. Zhang, X. Li, Y. Wang, *Applied Catalysis B Environmental* 168–169(2015) 472-482.

© 2016 The Authors. Published by ESG (www.electrochemsci.org). This article is an open access article distributed under the terms and conditions of the Creative Commons Attribution license (<http://creativecommons.org/licenses/by/4.0/>).